

Confinement enhancing barriers for high performance quantum dots-in-a-well infrared detectors

A. V. Barve, S. Sengupta, J. O. Kim, Y. D. Sharma, S. Adhikary, T. J. Rotter, S. J. Lee, Y. H. Kim, and S. Krishna

Citation: [Applied Physics Letters](#) **99**, 191110 (2011); doi: 10.1063/1.3660317

View online: <http://dx.doi.org/10.1063/1.3660317>

View Table of Contents: <http://scitation.aip.org/content/aip/journal/apl/99/19?ver=pdfcov>

Published by the [AIP Publishing](#)

Articles you may be interested in

[Optical pumping as artificial doping in quantum dots-in-a-well infrared photodetectors](#)

Appl. Phys. Lett. **94**, 053503 (2009); 10.1063/1.3073048

[High quantum efficiency dots-in-a-well quantum dot infrared photodetectors with AlGaAs confinement enhancing layer](#)

Appl. Phys. Lett. **92**, 193506 (2008); 10.1063/1.2926663

[Influence of quantum well and barrier composition on the spectral behavior of InGaAs quantum dots-in-a-well infrared photodetectors](#)

Appl. Phys. Lett. **91**, 173508 (2007); 10.1063/1.2802559

[Normal-incidence InAs / In 0.15 Ga 0.85 As quantum dots-in-a-well detector operating in the long-wave infrared atmospheric window \(8–12 \$\mu\text{m}\$ \)](#)

J. Appl. Phys. **96**, 1036 (2004); 10.1063/1.1760832

[High-responsivity, normal-incidence long-wave infrared \(\$\lambda 7.2\mu\text{m}\$ \) InAs / In 0.15 Ga 0.85 As dots-in-a-well detector](#)

Appl. Phys. Lett. **81**, 1369 (2002); 10.1063/1.1498009

An advertisement for COMSOL Multiphysics simulation projects. The background is dark with a grid pattern. On the left, there is a 3D cutaway view of a cylindrical component with a red interior and a blue exterior, showing a rainbow-colored light beam passing through a central hole. The text 'Over 600 Multiphysics Simulation Projects' is written in large, white, sans-serif font. Below the text, there is a blue button with the text 'VIEW NOW >>'. In the bottom right corner, the COMSOL logo is displayed, consisting of a small square icon followed by the word 'COMSOL' in white, sans-serif font.

Confinement enhancing barriers for high performance quantum dots-in-a-well infrared detectors

A. V. Barve,¹ S. Sengupta,¹ J. O. Kim,¹ Y. D. Sharma,¹ S. Adhikary,¹ T. J. Rotter,¹ S. J. Lee,² Y. H. Kim,² and S. Krishna^{1,a)}

¹Center for High Technology Materials, Department of Electrical and Computer Engineering, University of New Mexico, Albuquerque, New Mexico 87106, USA

²Korean Research Institute of Standards and Science, Daejeon 305340, South Korea

(Received 1 September 2011; accepted 24 October 2011; published online 11 November 2011)

We demonstrate the use of thin AlGaAs barrier layers in the quantum dots in a well heterostructure to enhance the quantum confinement of carriers in the excited energy level, while maintaining high escape probability. This is achieved by controlling the excited state energy between the confinement enhancing (CE) barriers and the continuum level. Responsivity of ~ 0.1 A/W, detectivity of 6.5×10^{10} cmHz^{1/2} W⁻¹ (77 K, 0.6 V, 7.5 μ m, $f/2$), and a factor of 10 improvement over a control sample without the CE barriers have been measured. The effect of changing the quantum well thickness and quantum dot size is also reported. © 2011 American Institute of Physics. [doi:10.1063/1.3660317]

Quantum dot infrared photodetectors (QDIPs) (Refs. 1–3) are promising candidates for the third generation focal plane arrays (FPAs) due to their high operating temperature,^{4–7} large area uniformity,^{8,9} and multicolor, bias tunable response.¹⁰ Self-assembled growth of quantum dots (QDs) in Stranski-Krastanov (SK) growth mode makes it difficult to control the peak wavelength and spectral properties of QDIPs. Quantum dots-in-a-well (DWELL) designs, in which InAs/InGaAs quantum dots are embedded in InGaAs/GaAs/AlGaAs quantum wells (QWs), solve this problem, making it easy to control the peak wavelength¹¹ as well as the width of the spectral response.⁷ However, since the infrared absorption in DWELL detectors, especially for midwave infrared (MWIR) wavelengths, results from ground state of the quantum dots to a higher lying excited state in the quantum well or to the continuum, the wavefunction overlap between the two states is low. This results in low absorption coefficients.

In this work, we use confinement enhancing (CE) AlGaAs barriers to increase the absorption coefficient, while maintaining high escape probability. The CE barriers are designed such that the excited energy in the QW is close to the continuum energy level, such that photoexcited electrons can easily escape. A similar concept was first demonstrated for quantum well infrared photodetectors (QWIPs), both theoretically¹² and experimentally.¹³ These type of bound to quasi-continuum (B-Q) transitions combine the advantages of bound to bound (B-B) transitions, such as high absorption efficiency and lower dark current,⁷ and bound to continuum (B-C) transitions, such as high escape probability and low bias operation. DWELL structures, where the quantum dot ground state and the quantum well excited state can be controlled independently, are ideal for designing architectures for B-Q transitions for a given wavelength, without reducing the barrier energy. The use of thin AlGaAs barriers around the DWELL region was previously reported¹ for the reduction in the dark current, but not for B-Q transitions. Ling

*et al.*¹⁴ suggested using a thin AlGaAs layer directly after the QD growth to confine the carriers in the lateral direction. However, AlGaAs layer does not conform the QD, due to the preferential growth of the AlGaAs layer away from InAs quantum dots. Thus, the barrier is presented only in the lateral direction, which does not result in decrease in the dark current. In the present architecture, CE barriers are grown such that they surround the entire DWELL structure, without altering the QD ground state energy. This results in reduced dark current due to the presence of a barrier in the transport direction.

Fig. 1(a) shows the heterostructure schematic of the CE DWELL 1 device and the DWELL control device which has the same structure without CE barriers. The devices were grown with elemental source molecular beam epitaxy with a valved arsenic cracker that supplies As₂. The active region consists of 7 DWELL layers, separated by 50 nm Al_{0.07}Ga_{0.93}As barriers. The DWELL region consists of Al_{0.2}Ga_{0.8}As (2 nm), GaAs (1 nm), In_{0.15}Ga_{0.85}As (1 nm), InAs QD (2.0 ML), In_{0.15}Ga_{0.85}As (4.2 nm), GaAs (1 nm), and Al_{0.2}Ga_{0.8}As (2 nm) layers for the CE DWELL 1 device. Material composition and thicknesses of each layer were chosen such that the excited energy is close to the continuum energy for optimum B-Q operation. To ensure a conformal coverage of CE barriers around the DWELL region, the following growth scheme was adopted: First, the barrier and CE barrier were grown and capped with 1 nm GaAs layer at 590 °C, before reducing the temperature to 500 °C to grow the In_{0.15}Ga_{0.85}As QW and 2 ML InAs QD doped with Si. After the QW growth, the structure was capped with 1 nm GaAs before changing the substrate temperature to 590 °C. This results in evaporation of excess InAs not capped by GaAs, thus forming a truncated pyramid. The substrate temperature was changed during a growth interrupt of 180 s. This insures that the 2 nm Al_{0.2}Ga_{0.8}As CE barrier is grown on a flat surface, which was also confirmed by observing the RHEED pattern changing from the chevron pattern associated with QD to a streak pattern, before the growth of CE barrier. Conformal coverage of CE barriers around the

^{a)}Author to whom correspondence should be addressed. Electronic mail: skrishna@chtm.unm.edu.

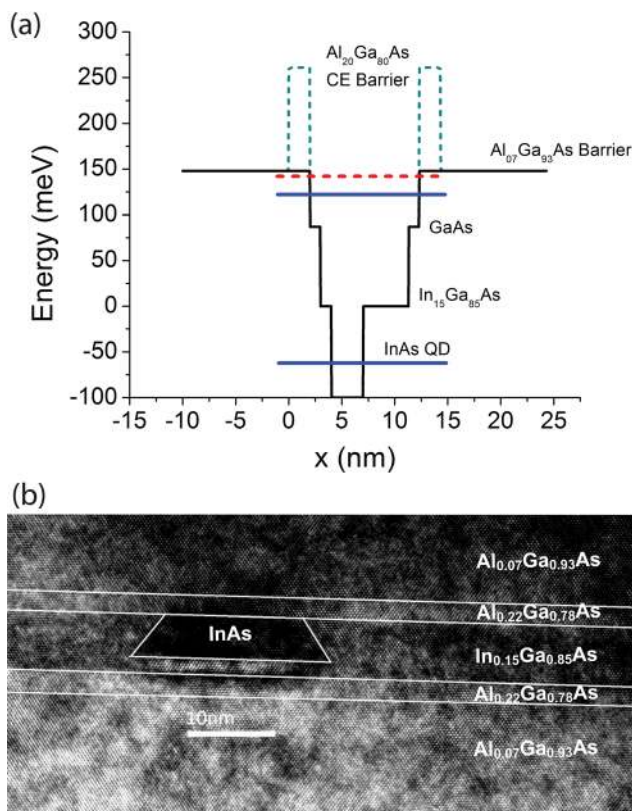


FIG. 1. (Color online) (a) Schematics of CE DWELL 1 and the DWELL control device active region, showing the influence of CE barrier (dashed) on the excited energy level, pushing it towards the continuum energy. (b) TEM image of DWELL region of CE DWELL 1. Truncated pyramidal InAs QD, InGaAs QW are clearly seen. CE Barriers encompass the DWELL region. Strain fields of quantum dot above and below the dot are visible.

DWELL regions and a truncated pyramidal QD can be observed in the high resolution tunneling electron microscope (TEM) image shown in Fig. 1(b). The contrast between $\text{Al}_{0.2}\text{Ga}_{0.8}\text{As}$ and $\text{Al}_{0.07}\text{Ga}_{0.93}\text{As}$ barriers is not high, due to a small strain mismatch between these layers.

Fig. 2(a) compares the spectral response obtained from CE DWELL device and the DWELL control device. The peak near $6.5\ \mu\text{m}$ is broader in CE DWELL device as compared to the control device. The $10.2\ \mu\text{m}$ peak present in the control device is completely blocked by the CE barrier, as it is bound deep in the QW. Figure 2(b) shows the spectral response obtained from the CE DWELL device at different temperatures, indicating that the ratio of the photocurrent at $6\ \mu\text{m}$ and $7.5\ \mu\text{m}$ decreases at higher temperatures. This indicates that the peak at $7.5\ \mu\text{m}$ probably results from the second excited state of the QD to the excited state in the QW.

The responsivity for the two devices, measured using a calibrated blackbody setup has been compared in Fig. 3(a) It is to be noted that for low bias, the responsivity is higher in CE DWELL device as compared to the control DWELL device, despite the addition of barriers. This indicates higher absorption efficiency and escape probability for the photoexcited electrons, even near zero bias. The CE barriers also reduce the dark current in the device by close to a factor of 10 at 77 K. This increase in the signal and reduction in the dark current results in a factor of 10 improvement in the detectivity for CE DWELL, as compared to the DWELL control device

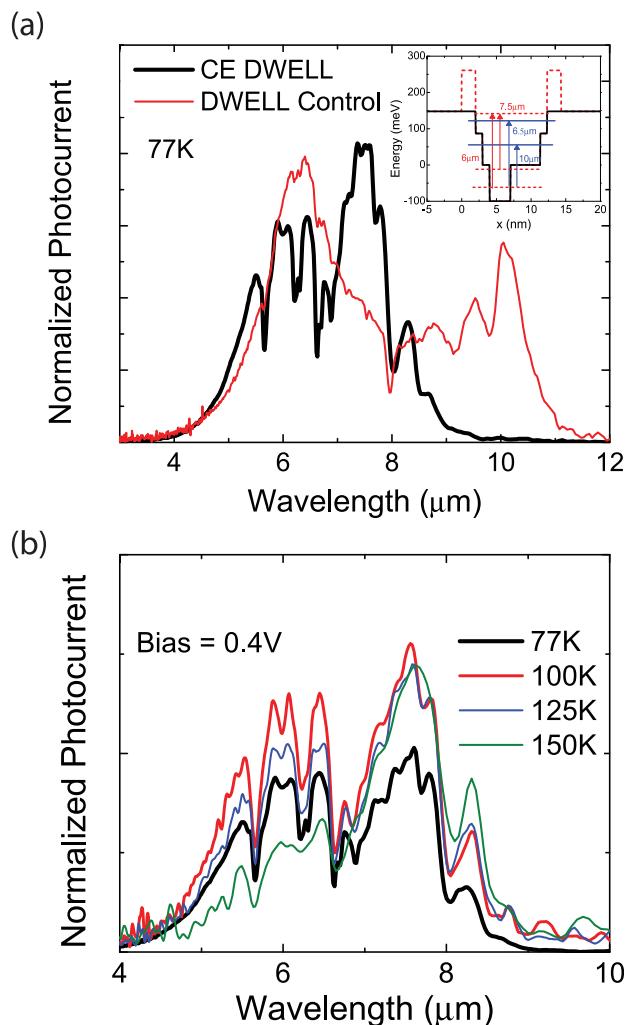


FIG. 2. (Color online) (a) Spectral response comparison between CE DWELL 1 and the DWELL control device at 77 K, showing broadening of the peak near $6.2\ \mu\text{m}$ and elimination of the bound to bound type peak at $10.2\ \mu\text{m}$ in CE DWELL 1 as compared to the DWELL control sample. Inset shows the schematics of participating transitions. (b) Spectral response from CE DWELL 1 at various temperatures, showing the ratio of peaks at $7.5\ \mu\text{m}$ and $6.2\ \mu\text{m}$ increases with temperature.

at 77 K, as shown in Fig. 3(b). Note that very high values of detectivities are obtained, even at zero bias. The detectivity is underestimated at zero bias due to the system noise in the noise measurement setup.

By changing the quantum well thickness or the quantum dot size, it is possible to change the response wavelength of the CE DWELL detectors. Fig. 4 shows the effect of change in QW thickness and QD size, respectively. CE DWELL 2 has $5.1\ \text{nm}$ InGaAs QW capping instead of $4.2\ \text{nm}$ in CE DWELL 1. This decreases the excited state energy by approximately $10\ \text{meV}$, as seen by the redshift in spectral response wavelength, as compared to CE DWELL 1. CE DWELL 3 has a same structure as CE DWELL 2 except for the $2.3\ \text{ML}$ nominal deposition of InAs QD instead of $2.0\ \text{ML}$ used in the other three structures. Formation of larger quantum dots, indicated by a redshift in PL by $\sim 45\ \text{meV}$, lowers the quantum dot ground state energy and the excited state energy in the quantum well. This results in bound to bound transitions, with a blueshift in spectral response. It is to be noted that all the structures with CE barriers completely suppress the B-B type peak at $10.2\ \mu\text{m}$, which is present in the control sample.

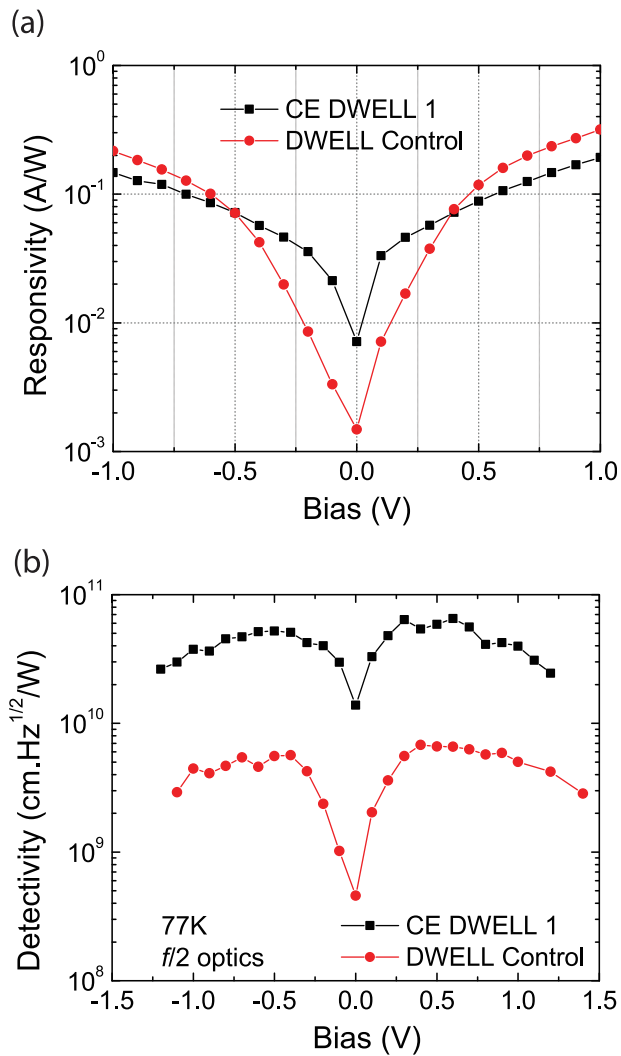


FIG. 3. (Color online) (a) Measured responsivity comparison between CE DWELL 1 and the DWELL control device at 77 K, showing a factor of 7 increase in responsivity for CE DWELL 1 at lower bias. (b) Measured detectivity of CE DWELL 1 device showing more than a factor of 10 increase in D^* over the DWELL control device, at 77 K, $f/2$ optics.

Although it is possible to alter the response wavelength by only changing the QW or the QD properties, this does not result in the excited state in QW close to the continuum energy. Thus, these devices fail to completely utilize the potential of confinement enhancing barriers, which results in a lower responsivity in these structures. However, due to the dark current reduction by the CE barriers, the noise also gets reduced, which compensates for the reduction in the responsivity. The measured peak detectivity is 2×10^{10} cmHz^{1/2}/W for CE DWELL 2 device and 1.8×10^{10} cmHz^{1/2}/W for CE DWELL 3 device, which is still a factor of 3 higher than that of the DWELL control device, but lower than that of CE DWELL 1 device, primarily because of the reduction in the responsivity.

In conclusion, an optimum design for confinement enhancing AlGaAs barriers for DWELL detectors has been presented, which exhibit higher signal and lower noise as compared to the control sample at low operating bias. A fac-

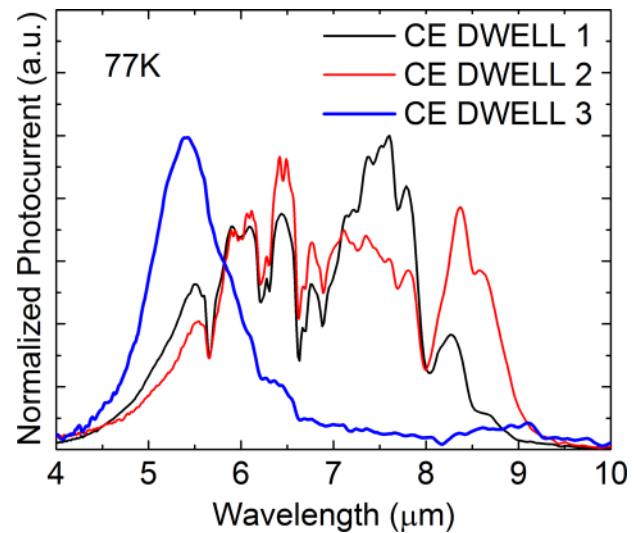


FIG. 4. (Color online) (a) Effect of QW thickness on the spectral response of CE DWELL structure, showing a redshift in the response due to 0.9 nm increase in the QW thickness for CE DWELL 2 device, and, the effect of QD nominal coverage, showing a blueshift in the spectral response in CE DWELL 3, which has 2.3 ML QD, as compared to 2.0 ML QDs in CE DWELL 2. B-B nature of transitions is clear from the small spectral width.

tor of 10 improvement in D^* , along with a strong near-zero bias response, indicates the successful operation of CE barriers. CE Barriers are grown such that they conformally cover the DWELL region, as indicated by TEM images. Effect of changing in QW and QD thickness has been studied. The B-B types of transitions resulting from non-optimum CE barrier designs reduce both signal and noise and show a factor of 5 improvement in the detectivity, as compared to the control sample.

This work is supported by AFOSR FA9550-09-1-0410, PST-2010-136, and KRIS-GRL Program.

¹J. C. Campbell and A. Madhukar, *Proc. IEEE* **95**(9), 1815 (2007).

²D. Stiff-Roberts, *J. Nanophotonics* **3**, 031607 (2009).

³V. Barve, S. J. Lee, S. K. Noh, and S. Krishna, *Laser Photonics Rev.* **4**(6), 738 (2010).

⁴P. Bhattacharya, S. Xiaohua, G. Ariyawansa, and A. Perera, *Proc. IEEE* **95**, 1828 (2007).

⁵H. Lim, S. Tsao, W. Zhang, and M. Razeghi, *Appl. Phys. Lett.* **90**, 131112 (2007).

⁶S. Tsao, H. Lim, W. Zhang, and M. Razeghi, *Appl. Phys. Lett.* **90**, 201109 (2007).

⁷A. V. Barve, Y. D. Sharma, T. J. Rotter, S. J. Lee, and S. K. Noh, *Appl. Phys. Lett.* **97**, 061105 (2010).

⁸S. D. Gunapala, S. V. Bandara, C. J. Hill, D. Z. Ting, J. K. Liu, S. B. Rafol, E. R. Blazejewski, J. M. Mumolo, S. A. Keo, S. Krishna, *et al.*, *IEEE J. Quantum Electron.* **43**, 230 (2007).

⁹D. Z. Y. Ting, S. V. Bandara, S. D. Gunapala, J. M. Mumolo, S. A. Keo, C. J. Hill, J. K. Liu, E. R. Blazejewski, S. B. Rafol, and Y. C. Chang, *Appl. Phys. Lett.* **94**, 111107 (2009).

¹⁰A. V. Barve, J. Shao, Y. Sharma, T. Vandervelde, K. Sankalp, S. J. Lee, S. K. Noh, and S. Krishna, *IEEE J. Quantum Electron.* **46**, 1105 (2010).

¹¹S. Krishna, *J. Phys. D* **38**, 2142 (2005).

¹²M. S. Kiledjian, J. N. Schulman, and K. L. Wang, *Phys. Rev. B* **44**(11), 5616 (1991).

¹³B. F. Levine, *J. Appl. Phys.* **74**, R1 (1993).

¹⁴H. S. Ling, *Appl. Phys. Lett.* **92**, 193506 (2008).